

Spectroscopy of Hydrothermal Reactions. 24. Kinetics of Alkyl Azide Decomposition Channels and N_3^- Behavior in Water above 200 °C at 275 Bar

Davide Miksa and Thomas B. Brill*

Department of Chemistry and Biochemistry, University of Delaware, Newark, Delaware 19716

Received: November 8, 2002; In Final Form: February 26, 2003

The hydrothermolysis of the water-soluble alkyl azide dimethyl-2-azidoethylamine (2-DAMEZ) was studied at 200–250 °C and 275 bar in real time by flow reactor FTIR spectroscopy. The kinetics of 2-DAMEZ decomposition by N_3^- formation represents a minor channel (8% at 250 °C). The main channel is loss of N_2 whose presence was determined by mass spectrometry. The Arrhenius parameters for decomposition by the two routes are $E_a = 14.1$ kcal/mol and $\ln(A, s^{-1}) = 10.7$ for the N_2 channel and $E_a = 17.4$ kcal/mol and $\ln(A, s^{-1}) = 11.8$ for the N_3^- channel. Because of further reactions the organic products could not be identified, but $(CH_3)_3N$ appears to be a major product. The N_3^- ion was found to be stable in water at least to 340 °C. However, protonation of N_3^- to form HN_3 was pH dependent. ΔH values for the reaction were calculated from a van't Hoff plot. It was found that changes in the bulk dielectric constant affect the equilibrium more than do changes in K_w in the 300–340 °C range. Ion pairing of NaN_3 and LiN_3 was also spectrally observed.

Introduction

The hydrothermolysis chemistry of the organoazide group has not been previously described. Such a determination requires that the compound be somewhat soluble in H_2O and that it decompose without uncontrollably releasing its energy. To this end, a study of dimethyl-2-azidoethylamine [(CH_3)₂NCH₂CH₂N₃ or 2-DAMEZ] was undertaken. The presence of the amine group renders solubility of 2-DAMEZ in H_2O to the extent of about 15 wt %.¹ Neat 2-DAMEZ has been proposed as a hypergolic liquid or gel fuel to replace methyl-substituted hydrazines in rocket propellants.² Although 2-DAMEZ is an energetic compound, its hydrothermal reactions could be studied spectroscopically in a flow reactor above 200 °C by use of a dilute aqueous solution.

By far the most common thermal decomposition pathway of an alkyl azide is the formation of N_2 and the nitrene, according to³



The presence of an electron-withdrawing group in the β -position, however, enhances the tendency to release HN_3 as well.^{4,5} The hydrothermal decomposition reaction of 2-DAMEZ occurred above 200 °C at 275 bar and gave evidence that the organoazide group liberated N_3^- as well as N_2 . This suggests that water enhances the possibility of two decomposition channels for 2-DAMEZ, although the question arises as to whether hydrothermolysis of N_3^- might be the source of N_2 . Therefore, the kinetics of the reaction channels of 2-DAMEZ leading to N_3^- and N_2 , as well as the hydrothermal behavior of the N_3^- ion, were characterized in this paper primarily by IR spectroscopy in real time at hydrothermal conditions. ¹H and ¹³C NMR spectroscopy recorded on the aqueous solution cooled and depressurized to room conditions aided in understanding the potential decomposition pathways of 2-DAMEZ.

Experimental Section

A sample of 2-DAMEZ⁶ was generously supplied by Drs. A. Manzara and R. Hunter of 3M Co., St. Paul, MN. (Dimethylamino)acetonitrile [(CH_3)₂NCH₂CN], dimethylethanolamine [(CH_3)₂NCH₂CH₂OH], and the unsymmetrical dimethylethylenediamine [(CH_3)₂NCH₂CH₂NH₂] were all commercially available from Aldrich, as were LiN_3 and NaN_3 . At a concentration of 0.25 *m* in 18 M Ω water, 2-DAMEZ can be studied because both the azide group intensely absorbed in the IR region and the heat liberated can be managed controllably. LiN_3 and NaN_3 were also investigated as 0.25 *m* solutions.

The kinetics of conversion of 2-DAMEZ to the N_3^- and the behavior of N_3^- (as NaN_3) in water were determined by the use of an optically accessible flow cell, which is described elsewhere.^{7,8} Briefly, the cell was constructed of grade 2 Ti and possessed 0° sapphire windows separated by a gold-foil washer having a thickness of about 20 μ m. The washer created the flow path for the transmission IR spectral observation and maintained a constant path length throughout the experiment. The controls on the flow reactor enabled a constant, known temperature (± 1 °C), pressure (± 1 bar) and flow rate (± 0.01 mL/min) to be maintained at all times. The solution was pumped through the cell against a static pressure of 275 bar by the use of an Isco syringe pump. A series of flow rates were used at 10 deg temperature increments in the 200–250 °C range. Transmission IR spectra were recorded at 4 cm^{-1} resolution by the use of a Nicolet 560 FTIR spectrometer. Thirty-two scans were combined at each condition.

Kinetics data for 2-DAMEZ were extracted from the area of the azide stretching absorbance (2116 cm^{-1} at 25 °C and 2108 cm^{-1} at 200 °C) as a function of the residence time and temperature. The area was obtained by fitting the peak with a four-parameter Voigt function using Peakfit (Jandel Scientific). To convert these areas into concentrations, it is necessary to know that the natural absorptivity of the azide mode does not change with temperature. If it does not, then the area change will directly reflect the reaction rate. Figure 1 shows that the

* Correspondence author. E-mail: brill@udel.edu.

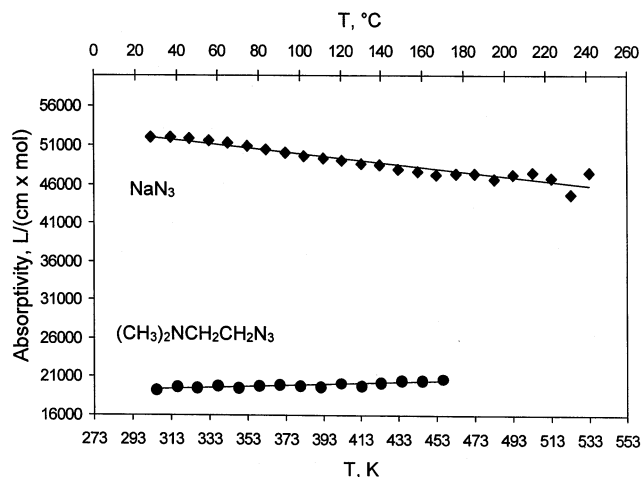


Figure 1. Comparison of the absorptivity for the N_3 stretching mode of 2-DAMEZ and free N_3^- in water over the 20–240 °C temperature range under 275 bar.

area of the azide absorbance in the 25–200 °C range is slightly dependent on the temperature. This result contrasts with the behavior of the neutral isoelectronic molecules CO_2 and N_2O whose absorptivities at constant concentration in water must be corrected at each temperature.⁹ Also shown in Figure 1 are the absorptivity values for the asymmetric stretching mode of aqueous N_3^- . Although the absorptivity of N_3^- was determined over the 20–240 °C temperature range, that of 2-DAMEZ could only be determined up to 170 °C before measurable decomposition occurred. Therefore, the absorptivity for 2-DAMEZ was extrapolated into the temperature range of interest. As can be seen from Figure 1, the absorptivity of free N_3^- is approximately 2.2 times greater than that of 2-DAMEZ in the 200–250 °C range. All of the experiments were run in triplicate, and the results were averaged.

Tube reactions in the batch mode followed by gas collection and mass spectrometry were employed to validate the presence of the N_2 from 2-DAMEZ.¹⁰ The ^1H NMR spectra of the cooled aqueous solutions were recorded at room conditions on a Bruker AM 250 spectrometer and referenced to H_2O set at 4.76 ppm so as to be comparable to shifts relative to TMS. TMS is of course not soluble in H_2O . About 5% D_2O was added to permit signal locking. The ^{13}C NMR spectra were recorded on a Bruker WM-400 spectrometer. The IR spectra taken at room conditions were recorded with a short path length ZnSe cell.

Results and Discussion

Spectra Analysis. IR spectra on 0.25 *m* solutions of 2-DAMEZ were recorded with different flow rates in 10 deg increments in the 200–250 °C range under a static pressure of 275 bar. Figure 2 shows selected spectra in the 1900–3000 cm^{-1} range as a function of the residence time at 220 °C. The intense $-\text{N}_3$ absorbance at 2109 cm^{-1} is replaced by the ionic azide absorbance at 2042 cm^{-1} . The C–H stretching region remains unchanged during the reaction, indicating that the $(\text{CH}_3)_2\text{N}-$ group is retained during the decomposition of the alkyl azide. Aqueous CO_2 is also present, as evidenced by the absorption at 2343 cm^{-1} . These products are easily understood as forming via C– N_3 bond fission to produce free N_3^- and the corresponding carbocation $(\text{CH}_3)_2\text{NCH}_2\text{CH}_2^+$ (eq 2), which reacted further to form eventually CO_2 among other products.

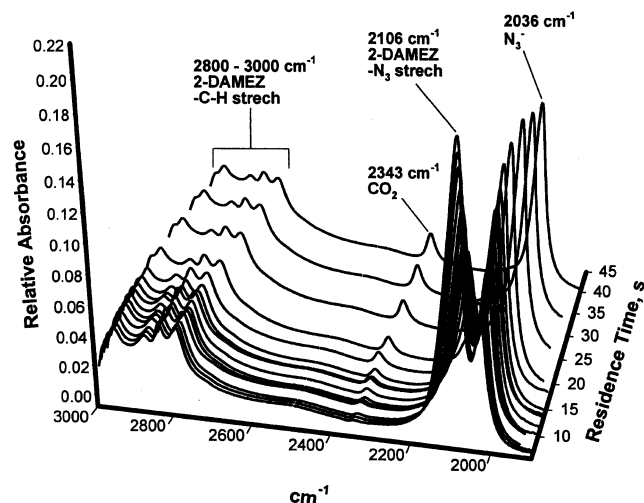
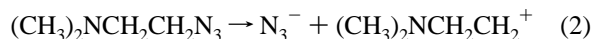


Figure 2. Spectral time series for the decomposition of 0.25 *m* 2-DAMEZ at 250 °C under 275 bar pressure.

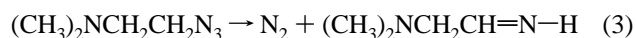
TABLE 1: Percent Decomposition Values for 2-DAMEZ and Percent Formation of N_3^- and CO_2 at the Indicated Temperatures

T , °C (residence time)	% 2-DAMEZ decomposition	% N_3^- formation	% CO_2 formation
200 ^a (42.9 s)	50	4	0.7 (210 °C)
250 ^a (40.1 s)	100	8.4	4

^a 0.1 mL/min.

Such observations do not address the extent of this reaction. A simple visual inspection of the spectra shown in Figure 2 cannot be used as the criterion to determine how much 2-DAMEZ decomposed to free N_3^- and coproducts because Figure 1 shows that the absorptivity of free N_3^- is approximately 2.2 times greater than that of 2-DAMEZ in the 200–250 °C range. The absorptivity data in Figure 1, however, enable the exact amount of free N_3^- in the spectra of Figure 2 to be determined. Also, the absorptivity data for aqueous CO_2 enable the amount of CO_2 to be determined.⁹ The degrees of conversion are summarized in Table 1, where it can be seen that at 250 °C only 8.4% of the azide appears as free N_3^- when all of the 2-DAMEZ is decomposed (Figure 2), and only 4% of the possible amount of CO_2 is present in solution. The decomposition of 2-DAMEZ via C– N_3 bond fission is therefore only a minor pathway.

Batch mode experiments of 0.25 *m* 2-DAMEZ in the titanium tube reactor at 260 °C afforded the gaseous products of the decomposition.¹⁰ Mass spectrometry of the collected gas revealed CO_2 and N_2 . Therefore, it was concluded that a second and the main decomposition pathway of 2-DAMEZ resulted in N_2 and an imine-like product (eq 3). H_2 was not detected, which eliminated the possibility of the ketenimine $(\text{CH}_3)_2\text{NCH}=\text{C}=\text{N}-\text{H}$ as a product.



To establish the identity of the imine product of eq 3, as well as the coproduct of N_3^- formation (eq 2), ^1H NMR spectra were taken of a 0.25 *m* 2-DAMEZ solution that had been heated in the titanium tube at 260 °C for 15 min (Figure 3). The simplicity and absence of multiplicity in the recorded signals indicated that the carbocation and the imine products of eqs 2 and 3, respectively, reacted further. Although the NMR spectrum was not ultimately assigned, some relevant conclusions can still be

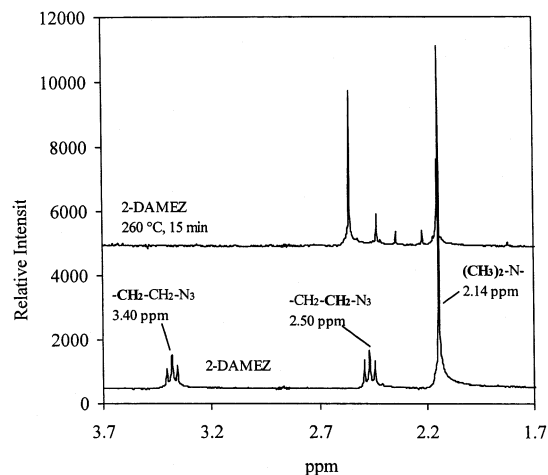
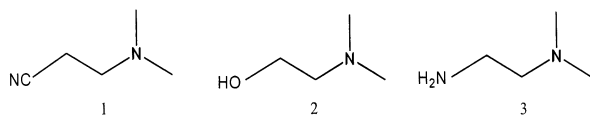


Figure 3. Comparison of ^1H NMR spectra for solutions of 0.25 *m* 2-DAMEZ reacted at 260 °C for 15 min and at room conditions.

derived from it. As mentioned earlier, the apparent absence of multiplicity indicates that no vicinal H atoms are present in the decomposition products. Furthermore, comparison of the reference ^1H NMR spectrum of 0.25 *m* 2-DAMEZ to that of the reacted solution at 260 °C reveals that the methylamine protons are retained in the product. This finding was also apparent in the IR spectra of Figure 2 where the C–H modes of the methyl group at 2800–3000 cm^{-1} do not change.

On the basis of these conclusions, compounds **1–3** seemed plausible as coproducts. However, none matched the NMR spectrum of the reacted 0.25 *m* 2-DAMEZ solution. J-Vert



measurements were also conducted and showed that the reacted solution was a mixture of products. ^{13}C NMR spectra were also difficult to interpret. Attempts to separate the product mixture by TLC using a variety of organic mobile phases failed. Tarlike products formed at longer reaction times, which made the solution increasingly heterogeneous.

The immediate coproduct of the C– N_3 fission reaction was postulated to be the $(\text{CH}_3)_2\text{NCH}_2\text{CH}_2^+$ carbocation (eq 2). Richard et al.¹¹ studied the spontaneous cleavage of a variety of *gem*-diazides to understand the kinetic and thermodynamic stability of carbocations in aqueous solutions. Despite their high reactivity, carbocations and the parent neutral species can equilibrate, so eq 2 might be written as an equilibrium. This possibility produced a worse fit with the kinetic model (vide infra) compared to considering only the forward reaction. Richard et al. also postulated that the carbocation should solvolyze to form the corresponding alcohol prior to being oxidized to the corresponding aldehyde. In the case of 2-DAMEZ, $(\text{CH}_3)_2\text{NCH}_2\text{CH}_2\text{OH}$ would form either via the carbocation or directly from nucleophilic attack by H_2O .

The ^1H NMR spectrum of dimethylethanolamine was inconsistent with Figure 3. Weak signals do appear in the 7.0–9.0 ppm region, which could correspond to the aldehyde proton in the above-mentioned structure. The aldehyde could then undergo nucleophilic attack by water and subsequently decarboxylate to the spectroscopically observed CO_2 (Figure 1) and $(\text{CH}_3)_3\text{N}$. To verify this hypothesis, the spectrum of $(\text{CH}_3)_3\text{N}$ solution through which CO_2 had been bubbled was also obtained. The methyl protons appear at 2.16 ppm, which is close to the 2.17

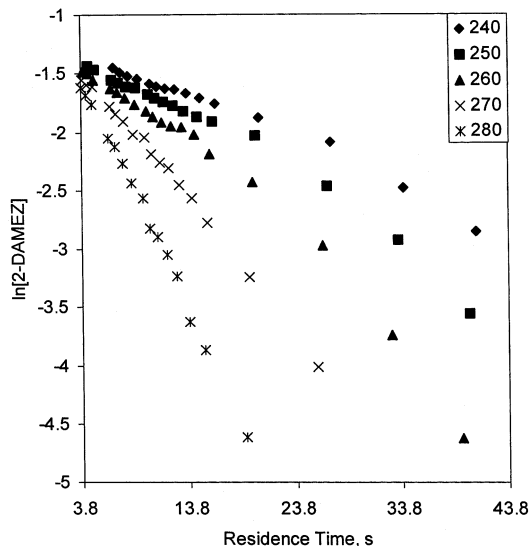


Figure 4. First-order rate plot for the decomposition of 2-DAMEZ over the 240–280 °C temperature range, based on the integration of the $-\text{N}_3$ absorbance located at 2106 cm^{-1} .

ppm signal of the reacted 2-DAMEZ. This observation is consistent with the IR spectra, which showed that the $(\text{CH}_3)_2\text{N}-$ group was preserved in the decomposition process.

Kinetics. Integration of the absorbances from spectral time series in Figure 2 afforded the rate plots (Figure 4) for decomposition of 2-DAMEZ and formation of free N_3^- . On the basis of the initial assumption that 2-DAMEZ decomposed according to two measurable pathways, a parallel reactions kinetic model was adopted:



where $A = [2\text{-DAMEZ}]$, $B = [\text{N}_3^-] + \text{coproducts}$, and $C = [\text{N}_2] + \text{coproducts}$. Because the kinetic data shown in Figure 4 are based on the overall decomposition of 2-DAMEZ, the corresponding rates are global (i.e., $k_{\text{obs}} = k_1 + k_2$). The concentration of free N_3^- and coproducts is given by

$$[B]_t = \frac{k_1[A]_0}{k} [1 - e^{-kt}] \quad (6)$$

where k is k_{obs} . Equation 6 was used to calculate a concentration profile that was compared to the profile obtained from integration of the free N_3^- absorbance located at 2036 cm^{-1} . Figure 5 shows that the fit is not perfect, which supports the existence of the parallel reactions. Because integration of the $-\text{N}_3$ stretching mode of 2-DAMEZ afforded the global rate of decomposition, and integration of the free N_3^- absorbance resulted in the rate of decomposition according to eq 3, it was possible to calculate the rate of 2-DAMEZ decomposition according to eq 3. First, however, the rate of free N_3^- formation was expressed in terms of 2-DAMEZ decomposition using the expression: $\ln([2\text{-DAMEZ}]_0 - [\text{N}_3^-]_t)$. Then $k_{\text{obs}} - k_1 = k_2$. The rate constants for 2-DAMEZ decomposition are summarized in the Arrhenius plot shown in Figure 6. The calculated values of k_2 (N_2 formation) are larger than the experimental k_1 values (N_3^- formation).

NaN_3 in the Hydrothermal Environment. Mentioned above was the possibility that hydrothermolysis of NaN_3 might be a source of N_2 and so a study of the stability of 0.25 *m* NaN_3

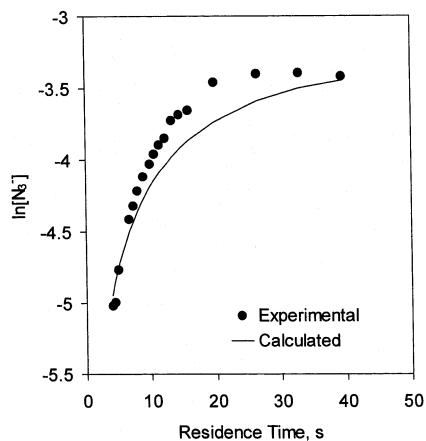


Figure 5. Comparison of the experimental versus the calculated concentration profile for free N_3^- based on eq 6.

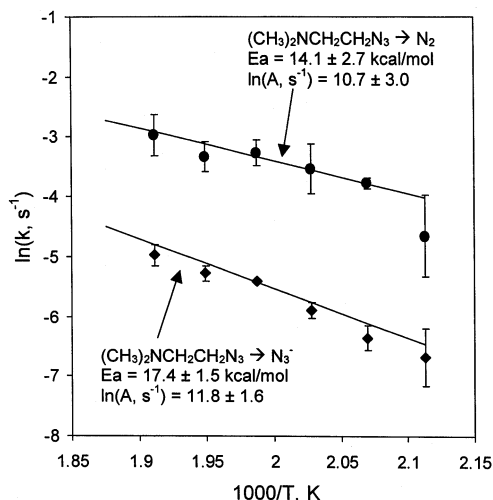
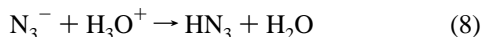
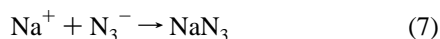
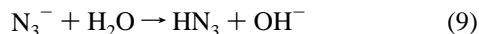


Figure 6. Comparison of the rates of 2-DAMEZ decomposition according to the N_2 formation pathway (k_2) versus the free N_3^- formation pathway (k_1) over 200–250 °C.

was undertaken at 300–340 °C. However, no change in the intensity of the N_3^- mode was found as a function of time. Instead, a strong pH dependence was seen. Because protonation of N_3^- leads to the weak acid HN_3 , the natural pH of a 0.25 *m* NaN_3 solution at room temperature is 9.3. At high temperatures eq 7 dominates at high pH, whereas eq 8 dominates at low pH.



The pH dependence of these equilibria is evident in Figure 7, which shows selected spectra for HN_3 , LiN_3 , and NaN_3 at 310 °C and different pH values. To quantify the influence of the properties of water on the intensities, these equilibria were investigated with respect to the ion product of water, K_w , and the bulk dielectric constant, ϵ . Equation 9 is the isoCoulombic



form of eq 8, which was used to predict the equilibrium constant for the N_3^-/HN_3 pair in the temperature range of interest. For comparison purposes $K_{\text{eq}25^\circ\text{C}} = 1.91 \times 10^{-5}$ and $K_{\text{eq}300^\circ\text{C}} = 4.54 \times 10^{-6}$.¹² The equilibrium shown in eq 8 incorporates the effects of K_w and ϵ and therefore does not permit the effect of each to be isolated. Instead, using the isoCoulombic eq 9 removes the

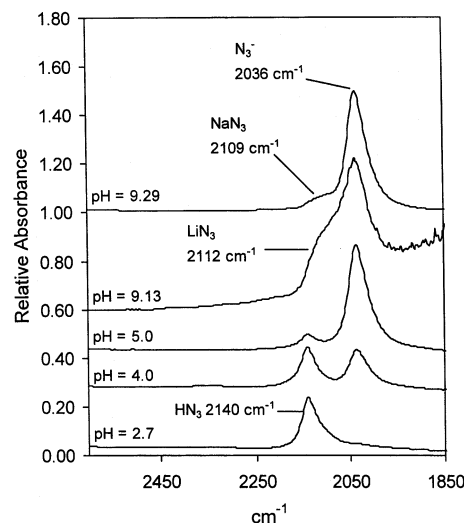


Figure 7. Spectral comparison of N_3^- , HN_3 , LiN_3 , and NaN_3 at 310 °C and the specified pH value. The absorptions of both the dissociated and undissociated forms are evident.

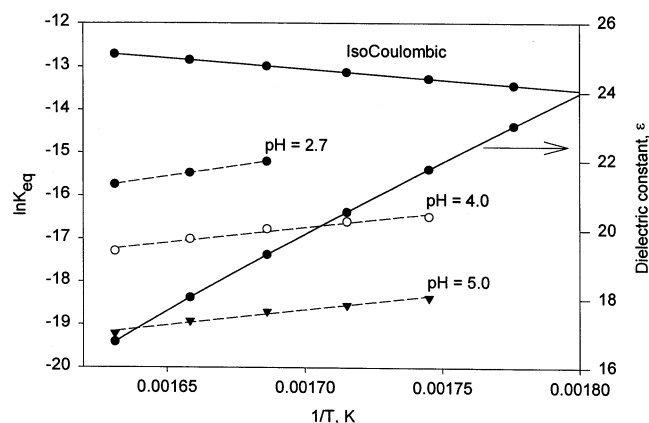


Figure 8. Van't Hoff plots for the N_3^-/HN_3 equilibria at different pH values as well as for the isoCoulombic equilibrium values (eq 5). The change in the dielectric constant of water over the same temperature range is also included.

effect of the dielectric constant, which allows the extrapolation to be a function of K_w alone. A van't Hoff plot was created (Figure 8) to compare the N_3^-/HN_3 equilibrium at different pH values. Also shown in Figure 9 is the change in the dielectric constant of water and the isoCoulombically calculated equilibrium constant. The extent of the influence of the dielectric constant of water on the N_3^-/HN_3 equilibrium compared to that of K_w , was determined with a fitting function

$$(\Delta \ln K_{\text{eq}} / \ln K_{\text{eq}}) = (1 - b) \frac{\Delta \epsilon}{\epsilon} + b \frac{\Delta K_w}{K_w} \quad (10)$$

K_{eq} was calculated using the concentrations of N_3^- and HN_3 measured from the IR spectra and ϵ and K_w are known.^{13,14} Table 2 summarizes the values of b for experiments conducted at different pH values over the 300–340 °C temperature range. As the temperature is increased, the influence of ϵ increases relative to the influence of K_w . However, the value of ϵ decreases, making the water field less able to support ions. Thus, NaN_3 and HN_3 favor their associated form, which is well-known for other salts.¹⁵ Also shown in Table 2 are the enthalpies of reaction from the van't Hoff plot for solutions of HN_3 at three values of the pH. The trend indicates an increase in exothermicity as the pH decreases because the equilibrium in eq 8 shifts

TABLE 2: Summary of Proportionality Values, b , According to Eq 10 and the Enthalpy of Reaction Values for Three Solutions Having Different pH Values at 300–340 °C

$T, ^\circ\text{C}$	b		
	pH = 2.7	pH = 4.0	pH = 5.0
300		0.22	0.23
310		0.21	0.22
320	0.17	0.20	0.20
330	0.16	0.18	0.18
340	0.13	0.15	0.15
$\Delta H, \text{kJ/mol}$	-81.0	-58.8	-60.3

TABLE 3: $\ln K_{\text{eq}}$ Values for a NaN_3 Solution (pH = 9.3 at 25 °C) at 290–330 °C^a

$T, ^\circ\text{C}$	$\ln K_{\text{eq}}$
290	-15.35
300	-15.50
310	-15.59
320	-15.56
330	-15.58
$\Delta H, \text{kJ/mol}$	-15.1

^a The corresponding ΔH of reaction was calculated on the basis of the van't Hoff plot.

to the right. The $\ln K_{\text{eq}}$ values for the NaN_3 solution at its natural pH of 9.3 are shown in Table 3. The corresponding ΔH value is consistent with the exothermicity trend shown in Table 2. The considerably lower ΔH value for NaN_3 is probably due to the weaker interaction between Na^+ and N_3^- compared to H^+ and N_3^- .

LiN_3 was investigated under the same temperature and pressure conditions used for the N_3^-/HN_3 study (Figure 8). As expected, the frequency of the azide stretch for association of LiN_3 occurs between those of the associated forms of HN_3 and NaN_3 .

Conclusions

IR spectroscopy and mass spectrometry support a dual mechanism involving (1) loss of nitrogen via $\text{CN}-\text{N}_2$ bond scission and formation of a reactive imine as the primary

decomposition channel and (2) loss of azide via cleavage of the $\text{C}-\text{N}_3$ bond as the secondary channel. A reactive carbocation is thought to be the coproduct in this second reaction. The fates of the coproducts of both decomposition channels were not well defined. There is evidence, however, that $(\text{CH}_3)_3\text{N}$ is an indirect product of 2-DAMEZ decomposition. Also, the observation of CO_2 in the IR spectra is consistent with a decarboxylation reaction possibly involving an aldehyde intermediate. The behaviors of HN_3 , LiN_3 , and NaN_3 in the hydrothermal environment were investigated to learn whether the azide ion decomposed as well. It was found that the equilibrium described by eq 8 dominates in the high-temperature regime and is influenced more by the dielectric constant of water than by K_w . The azide ion is, however, chemically unreactive at the conditions of the experiments.

Acknowledgment. We are grateful to the Army Research Office for support of this work on DAAG55-98-1-0253.

References and Notes

- (1) Manzara, A.; Hunter, R. 3M Co., personal communication, 1999.
- (2) Thompson, D. M. U.S. Patent 6,013,143, Jan. 11, 2000; *Chem. Abstr.* 132, 51978.
- (3) Bock, H.; Dammel, R. *Angew. Chem., Int. Ed. Engl.* **1987**, 26, 504.
- (4) Brill, T. B.; Karpowicz, R. J.; Haller, T. M.; Rheingold, A. L. *J. Phys. Chem.* **1984**, 88, 4139.
- (5) Oyumi, Y.; Rheingold, A. L.; Brill, T. B. *J. Phys. Chem.* **1987**, 91, 920.
- (6) Schiemenz, G. P.; Engelhard, H. *Chem. Ber.* **1959**, 92, 857.
- (7) Kieke, M. L.; Schoppelrei, J. W.; Brill, T. B. *J. Phys. Chem.* **1996**, 100, 7455.
- (8) Schoppelrei, J. W.; Kieke, M. L.; Wang, X.; Klein, M. T.; Brill, T. B. *J. Phys. Chem.* **1996**, 100, 14343.
- (9) Maiella, P. G.; Schoppelrei, J. W.; Brill, T. B. *Appl. Spectrosc.* **1999**, 53, 351.
- (10) Miksa, D.; Brill, T. B. *Ind. Eng. Chem. Res.* **2002**, 41, 5151.
- (11) Richard, J. P.; Amyes, T. L.; Jagannadham, V.; Lee, Y.; Rice, D. *J. Am. Chem. Soc.* **1995**, 117, 5198.
- (12) Kortüm, G.; Vogel, W.; Andrussow, K. *Dissociation Constants of Organic Acids in Aqueous Solution*; Butterworth: London, 1961.
- (13) Uematsu, M.; Franck, E. U. *J. Phys. Chem. Ref. Data* **1980**, 9, 1291.
- (14) Marshall, W. L.; Franck, E. U. *J. Phys. Chem. Ref. Data* **1981**, 10, 295.
- (15) Spohn, P. D.; Brill, T. B. *J. Phys. Chem.* **1989**, 93, 6224.